Supplementary material for:

Mineral compositions and thermobarometry of basalts and boninites recovered during IODP Expedition 352 to the Bonin forearc

SCOTT A. WHATTAM[1*], JOHN W. SHERVAIS[2], MARK K. REAGAN[3], DANIEL A. COULTHARD JR., JULIAN A. PEARCE[4], PETER JONES[5], JIEUN SEO[6], KEITH PUTIRKA[7], TIMOTHY CHAPMAN[8,9], DANIEL HEATON[10], HONGYAN LI[11], WENDY R. NELSON[12], KENJI SHIMIZU[13] AND ROBERT J. STERN[14]

[1]Department of Geosciences, King Fahd University of Petroleum and Minerals, Dhahran 31261, Saudi Arabia

[2]Department of Geology, Utah State University, Logan, UT 84322-4505, USA

[3]Department of Earth and Environmental Sciences, University of Iowa, Iowa City, IA 52242, USA

[4]School of Earth, Ocean and Planetary Sciences, Cardiff University, Cardiff CF10 3YE, UK

[5]Department of Earth Sciences, Carleton University, Ottawa, ON, K1S 5B6, Canada

[6]Department of Earth and Environmental sciences, Korea University, Seoul 02841, South Korea

[7]Department of Earth and Environmental Sciences, California State University, Fresno, CA 93740, USA

[8]School of Geosciences, University of Sydney, NSW 2006, Australia

[9]Earth Science, School of Environmental and Rural Science, University of New England, NSW 2351, Australia

[10]College of Earth, Ocean and Atmospheric Sciences, Oregon State University, Corvalis, OR 97331-5503, USA

[11]State Key Laboratory of Isotope Geochemistry, Guangzhou Institute of Geochemistry, Chinese Academy of Sciences, Guangzhou 510640, PR China

[12]Department of Physics, Astronomy and Geosciences, Towson University, Towson, MD 21252, USA

[13]Kochi Institute for Core Sample Research, Japan Agency for Marine-Earth Science and Technology, Monobe-otsu 200, Nankoku, Kochi, 783-8502, Japan

[14]Geosciences Department, University of Texas at Dallas, Richardson, TX 75083-0688, USA

SUPPLEMENTARY MATERIAL

Supplementary data comprises:

11-pg. Text Supplement:

Sections

Petrography
PetDB MORB and VAB sample selection and procedures and data manipulation
References

Supplemental Figures and Tables:

Figures S1
Tables S1-S12

* Corresponding author. Tel.: 011 91 765 706 9434
E-mail address: sawhatta@gmail.com; scott.whattam@kfupm.edu.sa

PETROGRAPHY

Forearc basalt and dolerite

FAB lavas, including rare vitrophyres, were recovered from Holes U1440A, B and U1441A (Figure 1b). Dolerites were recovered from U1440B where they comprise a probable sheeted dyke complex. The FAB are typically aphyric to sparsely augite-phyric, plagioclase-phyric or plagioclase-augite-phyric (Figure 3a, b). Plagioclase, augite and mesostasis constitute approximately 38%, 20%, and 15% of the mode, respectively (Table 1). The groundmass exhibits subophitic to insertal microcrystalline textures with ~0.2 mm subhedral plagioclase laths and $\leq$ 1.2 mm subhedral, blocky augite crystals set in a mesostasis of quench crystals ± glass (Table 2). Whereas in most cases the groundmass is completely altered and composed of oxidized cryptocrystalline, dark reddish-brown palagonite, plagioclase and clinopyroxene have largely escaped alteration. Secondary processes are also evident as veinlets filled with carbonates and zeolites which occupy up to 20% of some samples. Most FAB are not vesicular, but in some cases up to 10-15 modal % of subrounded and amorphous, unfilled vesicles are present (Table 1).

The vitrophyres are sparsely plagioclase- or plagioclase-augite-phyric and microphyric. Microphenocrysts occupy <1% of the mode and are tabular, euhedral and $\leq$ 0.8 mm. The groundmass of the vitrophyres constitutes $\geq$ 99% of the mode and consists of glass or devitrified glass with no vesicles.

The dolerites exhibit predominately subophitic but also intergranular, intersertal, and hypidiomorphic granular textures and are fine to medium grained (0.3-2.0 mm). Plagioclase occupies 45-50% of the mode and forms subhedral tabular grains with rare sieve texture. Augite encompasses approximately 30-40% of the mode and is manifest as subhedral, blocky to prismatic

grains which are commonly poikilitic (augite enclosing radiating laths of plagioclase set in a matrix of altered glass). Fe-Ti oxides comprise 1-2% of the mode and form small (0.1-0.3 mm) equant, interstitial grains. Small equant grains of (apparent) quartz and chloritic alteration products are found within the mesostasis of intersertal patches.

Andesite

The lone andesite is a sparsely augite-plagioclase-phyric, microcrystalline lava (Figures 3c, d) with ~2% augite and 1% plagioclase phenocrysts (Table 1). Augite phenocrysts are ~0.6 mm euhedral, prismatic crystals while plagioclase phenocrysts are ~0.4 mm subhedral, tabular laths with infrequent albite rims. The groundmass comprises ~40% microcrystalline, $\leq$ 0.2 mm tabular plagioclase and 57% mesostasis with about 3% vesicles.

High-Mg andesites

The high-Mg lavas are aphyric to sparsely or moderate augite-orthopyroxene-phyric, plagioclase-augite-phyric, olivine-augite-orthopyroxene phyric or olivine-plagioclase-augite-phyric (Figures 3e, f). Almost all lavas are fine-grained to microcrystalline and exhibit intersertal to intergranular textures; one sample is a vitrophyre. Apart from the vitrophyre, all lavas have a fine to microcrystalline groundmass dominated by plagioclase microlites and comprising plagioclase (25-55%), augite (8-25%), orthopyroxene (0-10%), and mesostasis (19-59%) (Table 1). All phenocrysts range from <0.5-4 mm with an average size of about 0.8 mm (Table 2).

Boninites

Basaltic and low silica boninites

The lone basaltic boninite is moderately olivine-augite-phyric whereas the low-Si boninites (Figures 3g, h) are highly to moderately olivine- to olivine-orthopyroxene or olivine-clinopyroxene-phyric. In the basaltic boninite and low-Si boninite, olivine typically occupies 0-20% and rarely up to 25-30% of the mode and in the low-Si boninite, orthopyroxene commonly comprises 1-2% of the mode but many samples are devoid of orthopyroxene phenocrysts (Table 1). Similarly, clinopyroxene which typically comprises 1-6% modally of the low-Si boninite, is commonly absent as a phenocryst phase. In the low-Si boninite, both pyroxenes range in size from ~0.2 to 0.8 mm in long dimension (~0.5 mm on average) and are typically euhedral and prismatic to blocky (Table 2). Groundmass of the low-Si boninite is either glass dominated (35-55% modal glass), mesostasis dominated (60-90% mesostasis) or crystalline with ~14% plagioclase, 20% clinopyroxene, 1% orthopyroxene, 2-3% opaque oxides and 15-50% mesostasis. The grain size of the low-Si boninite groundmass constituents is typically 0.1-0.4 mm and the grain size in the mesostasis is typically <<0.1 mm. Vesicles are absent in the lone basaltic boninite sample but average about 10% and range up to 40% in some mesostasis dominated low-Si boninite samples. Vesicles are rare to absent in most crystalline or glassy low-Si bonnites but vitrophyres have ~30% vesicles.

High-Si boninites

The high-Si boninites are highly to sparsely olivine-orthopyroxene-phyric (Figures 3i, j). Olivine typically comprises <1% of the mode but can compose up to 5-10% of samples. Orthopyroxene usually occupies about 0.5-4% of the mode but ranges up to 8-15% in highly phyric samples (Table 1). Olivine and orthopyroxene are ~0.1-1.6 mm long and are typically euhedral and prismatic to blocky (Table 2). Lavas with more crystalline groundmasses commonly have thin

rims of clinopyroxene overgrowths on orthopyroxene phenocrysts. The more crystalline groundmasses consists of acicular needles of orthopyroxene and clinopyroxene with typically ~ 46 % pale tan glass. Other lavas are essentially vitrophyres with 50-65% pale tan glass containing 4-20% phenocrysts and 25-40% microcrystalline pyroxene. The more crystalline lavas typically have up to ~15% vesicles while the vitrophyric lavas have about 2-6% vesicles. Though most samples have vesicles, some do not. Clasts of high-Si boninite have also been recovered in pyroclastic deposits. These clasts are identical to high-Si boninite lavas but typically have more vesicles.

PETDB MORB AND VAB SAMPLE SELECTION, PROCEDURES AND DATA MANIPULATION

PetDB MORB and VAB clinopyroxene sample collation

The following steps were taken at the Petrological Database website (PetDB, (http://www.earthchem.org/petdb) in order to build our dataset of PetDB MORB and VAB clinopyroxenes: Step 1: From the PetDB main menu we clicked PetDB Search from which we subsequently chose samples on the basis of *Tectonic Setting* from which we chose *Spreading Center* (Tectonic Setting = MORB was not an option) which returned 30701 samples. Step 2: We then chose *Sample Type* and limited our criteria to *Rock Type* → *igneous: volcanic: mafic* and selected *basalt* and *tholeiite* which returned 26338 samples. Step 3: We then continued to *Data Selection* where we chose *Mineral Analyses*, *Mineral Type = clinopyroxene* and of the *variables*, selected *Major Oxides* (only) which returned 1370 (clinopyroxene) analyses; we subsequently downloaded the dataset. Step 4: From the downloaded excel spreadsheet we then filtered samples such that only samples in which *Rock* (name) was either *BASALT, igneous: volcanic: mafic* or *THOLEIITE, igneous: volcanic: mafic*. Samples which were either left unnamed or contained a

name other than the above (e.g., *GABBRO, PERIDOTITE*) were removed as were samples which did not have oxide totals between 95-103 wt. %. This resulted in a dataset of 1173 MORB clinopyroxene analyses. Step 5: Total Fe as FeO cation proportion calculations were then performed whereby cation proportions were based on six oxygens for clinopyroxene. We followed identical procedures for VAB clinopyroxene analyses collation but with *Tectonic Setting* = *Volcanic Arc* which resulted in $n = 229$ clinopyroxene analyses and $n = 204$ clinopyroxene analyses subsequent to filtering as described above.

PetDB MORB samples chosen P-T estimates calculation: Dataset collation and data manipulation

As PetDB does not allow for a combined search of MORB whole-rock chemistry plus clinopyroxene mineral chemistry, we first obtained whole rock data for MORB but limited samples returned to those only with (complimentary) clinopyroxene mineral analyses available; we then performed a search for MORB clinopyroxene compositions (only) and matched samples from each dataset to construct a combined dataset of MORB samples with complimentary whole-rock and clinopyroxene compositions. Details of MORB sample selection and collation from PetDB are as follows: For whole-rock MORB sample selection: Step 1: We chose samples on the basis of *Tectonic Setting* from which we chose *Spreading Center*. Step 2: For *Rock Type* we chose *igneous: volcanic: mafic* and selected *basalt* and *tholeiite* which returned 1232 samples. Step 3: We then filtered *Sample Selection* via *Data Availability* → (only) those (whole-rock analyses) with (complimentary) clinopyroxene analyses. Step 4: For *Rock Analyses* we chose *one row per sample, major elements only*. For *Spreading Center* clinopyroxene analyses: Steps 1-3 were performed as above for whole-rock MORB selection. Step 4: On a second spreadsheet, we kept only the first

clinopyroxene composition listed for each sample. To combine the above MORB whole rock and MORB clinopyroxene datasets we: 1. On a separate spreadsheet in the clinopyroxene compositions spreadsheet, appended the list of clinopyroxene compositions by keeping the first analysis only and deleting the remainder. 2. On a separate sheet in the whole-rock compositions spreadsheet, we appended the list of whole-rock compositions such that when there were two duplicate analyses, presented - one of glass and one of whole-rock- only the first one listed (which was usually glass) was kept. 3. When clinopyroxene compositions were presented which did not provide a complimentary whole-rock composition in the whole-rock spreadsheet, these cpx compositions were deleted on the 'Data with one clinopyroxene listed per sample sheet'. 4. Similar to 3 immediately above, when whole-rock compositions were presented which did not provide a complimentary clinopyroxene composition in the clinopyroxene spreadsheet, these whole-rock compositions were deleted. 5. When the two aforementioned datasets were merged into one dataset with whole-rock and complimentary clinopyroxene compositions, data was culled such that only whole-rock compositions with SiO_2 = 45-52 wt. % and oxide totals = 98-102 wt. % were kept. Whole rock Mg was calculated assuming $Fe^{3+}/FeT = 0.17$ (Brounce et al., 2015) whereby $FeT = Fe^{2+}+Fe^{3+}$. Whole rock compositions were then normalized on a volatile-free basis. Finally, only clinopyroxene core or 'probable core' compositions were used in the calculation of P-T estimates (i.e., clinopyroxene rim compositions were ignored).

The original dataset of PetDB samples of MORB with complimentary clinopyroxene that we compiled consists of 181 samples; of these, 91 samples were ones in which clinopyroxene was deemed to be equilibrium with the liquid (whole rock) on the basis of the Mg# clinopyroxene vs. Mg# whole-rock relations (i.e., Rhodes diagram), see main text for further details). Of these remaining 91 samples we filtered data such that samples which yielded (a) clinopyroxene

compositions with missing oxides such that the predicted DiHd clinopyoxene component could not be calculated (i.e., predicted DiHd = 0) and (b) pressure estimates (of Neave and Putirka, 2017) less than or equal to -2 kbar were discarded. These filters left 75 remaining samples all of which fell within ±0.1 error of their observed/predicted compositions (Supplementary Figure S2).

Captions for Supplementary Figures and Tables

Supplementary Figure S1 Test for equilibrium plot using predicted vs. observed clinopyroxene components for (a) Expedition 352 FAB, (b) Expedition 352 anomalous andesite TS 93 and basaltic boninite, and (c) PetDB MORB. Note that in (c), one PetDB sample plots off the top of the plot with a predicted EnFs of ~1.2.

Supplementary Table S1 Correlation of informal thin section numbers (used in text) with IODP-assigned sample numbers.

Supplementary Table S2 Chemical compositions of clinopyroxene of low-Si and high-Si boninites, andesite, high-Mg andesites and FAB of Holes U1439C, U1442A, U1440B and U1441A.

Supplementary Table S3 Representative chemical compositions of orthopyroxene of low-Si and high-Si boninites and high-Mg andesites of Holes U1439C and U1442A.

Supplementary Table S4 Representative chemical compositions of olivine of low-Si and high-Si boninites of Holes U1439C and U1442A.

Supplementary Table S5 Representative chemical compositions of spinel of low-Si and high-Si boninites of Holes U1439C and U1442A.

Supplementary Table S6 Representative chemical compositions of magnetite of forearc basalts of Hole U1440B.

Supplementary Table S7 Representative chemical compositions of plagioclase of low silica boninites, andesite (TS 93), forearc basalts and forearc dolerites of Holes U1439C, U1442A, U1440A, U1440B and U1441.

Supplementary Table S8 P-T calculations based on clinopyroxene thermobarometry.

Supplementary Table S9 P-T calculations based on orthopyroxene thermobarometry.

Supplementary Table S10 T calculations based on olivine thermometry.

Supplementary Table S11 PetDB MORB samples in equilibrium and their P & T estimates on the basis of clinopyroxene thermobarometry.

Supplementary Table S12 Fugacity calculation for Expedition 352 boninites.

Supplementary Table S13 Boninite crystallization pressure and temperature estimates from the literature.

REFERENCES CITED

Beattie, P. (1993) Olivine-melt and orthopyroxene-melt equilibria. Contributions to Mineralogy and Petrology, 115, 103-111.

Neave, D. and Putirka, K. (2017) A new clinopyroxene-liquid barometer, and implications for magma storage pressures under Icelandic rift zones. American Mineralogist, 102, in press.

Putirka, K.D. (2008) Thermometers and barometers for volcanic systems. In: Putirka, K.D., Tepley, F. (Eds.), Reviews of Mineralogy and Geochemistry, 69, 61-120.

Putirka, K.D. (2016) Rates and styles of planetary cooling on Earth, Moon, Mars, and Vesta, using new models for oxygen fugacity, ferric-ferrous ratios, olivine-liquid Fe-Mg exchange, and mantle potential temperature. American Mineralogist, 101, 819-840.

Putirka, K., Johnson, M., Kinzler, R., and Walker D. (1996) Thermobarometry of mafic igneous rocks based on clinopyroxene-liquid equilibria, 0-30 kbar. Contributions to Mineralogy and Petrology, 123, 92-108.

Putirka, K.D., Perfit, M., Ryerson, F.J., and Jackson, M.G. (2007) Ambient and excess mantle temperatures, olivine thermometry, and active vs. passive upwelling. Chemical Geology, 241, 177-206. http://dx.doi.org/10.1016/j.chemgeo.2007.01.014.

Putirka, K., Ryerson, F. J., and Mikaelian, H. (2003) New igneous thermobarometers for mafic and evolved lava compositions, based on clinopyroxene + liquid equilibria. American Mineralogist, 88, 1542-1554.

Roeder, P.L., and Emslie, R.F. (1970) Olivine-liquid equilibrium, Contributions to Mineralogy and Petrology 29, 275-289.

Topliss, M.J., and Carroll, M.R. (1995) An experimental study of the influence of oxygen fugacity on Fe-Ti oxide stability, phase relations and mineral-melt equilibria in ferro-basaltic systems, Journal of Petrology, 36, 1137-1170.

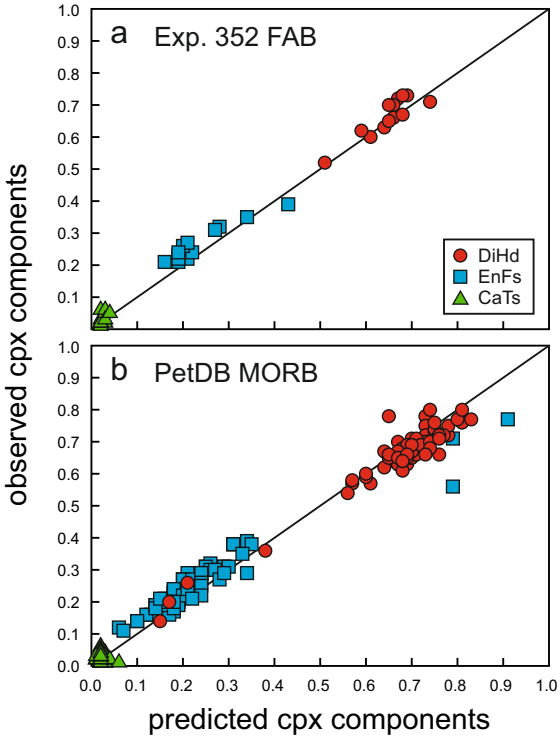

Supplementary Fig.1 Whattam et al. 2020

Supplementary Table S1 Correlation of informal thin section nos. (used in text) with IODP-assigned sample numbers

Rock Type	Our informal TS no.	Formal IODP no.
FAB	TS_25	352-U1440B-11R-1-W 12/15-TSB-TS_25
FAB	TS_35	352-U1440B-17R-1-W 14/15-TSB-TS_35
FAB	TS_45	352-U1440B-23R-1-W 29/32-TSB-TS_45
FAB	TS_50	352-U1440B-26R-1-W 64/67-TSB-TS_50
FAB	TS_70	352-U1440B-34R-1-W 132/134-TSB-TS_70
FAB	TS_72	352-U1440B-35R-1-W 32/35-TSB-TS_72
FAB	TS_73	352-U1440B-36R-1-W 4/7-TSB-TS_73
FAB	TS_164	352-U1441A-10R-1-W 29/31-TSB-TS_164
FAB	TS_176	352-U1441A-18R-1-W 33/37-TSB-TS_176
FAB	TS_180	352-U1441A-20R-1-W 39/41-TSB-TS_180
FAB	TS_178	352-U1441A-21R-1-W 34/37-TSB-TS_178
FAB	TS_172	352-U1441A-22R-1-W 8/11-TSB-TS_172
AND	TS_93	352-U1439C-8R-2-W 105/107-TSB-TS_93
HMA	TS_90	352-U1439C-7R-2-W 59/61-TSB-TS_90
HMA	TS_157	352-U1439C-42R-1-W 60/62-TSB-TS_157
HMA	TS_208	352-U1442A-34R-1-W 62/65-TSB-TS_208
HMA	TS_209	352-U1442A-35R-1-W 51/54-TSB-TS_209
BB	TS_102	352-U1439C-13R-2-W 22/25-TSB-TS_102
LSB	TS_105	352-U1439C-15R-1-W 130/133-TSB-TS_105
LSB	TS_110	352-U1439C-18R-2-W 105/108-TSB-TS_110
LSB	TS_111	352-U1439C-19R-3-W 55/58-TSB-TS_111
LSB	TS_119	352-U1439C-23R-2-W 22/24-TSB-TS_119
LSB	TS_137	352-U1439C-32R-1-W 98/101-TSB-TS_137
LSB	TS_151	352-U1439C-40R-1-W 36/38-TSB-TS_151
LSB	TS_191	352-U1442A-23R-1-W 103/105-TSB-TS_191
LSB	TS_203	352-U1442A-30R-2-W 27/30-TSB-TS_203
HSB	TS_80	352-U1439C-2R-3-W 38/41-TSB-TS_80
HSB	TS_88	352-U1439C-5R-1-W 92/95-TSB-TS_88
HSB	TS_89	352-U1439C-6R-1-W 30/31-TSB-TS_89
HSB	TS_182	352-U1442A-11R-1-W 75/77-TSB-TS_182
HSB	TS_183	352-U1442A-13R-1-W 6/9-TSB-TS_183
HSB	TS_185	352-U1442A-15R-1-W 72/74-TSB-TS_185
HSB	TS_188	352-U1442A-20R-1-W 104/106-TSB-TS_188
HSB	TS_196	352-U1442A-25R-1-W 80/83-TSB-TS_196

Abbreviations:FAB, forearc basalt; AND, andesite; HMA, high-Mg andesite; BB, basaltic boninite; LSB, low-Si boninite; HSB, high-Si boninite

Supplementary Table S2 Chemical compositions of clinopyroxene

Page 3 of 4

Page 4 of 4

| Core locus | A42PC | | |

Supplementary Table S3 Chemical compositions of orthopyroxene

Sample																																			
Drill hole											**U1439C**																		**U1442A**							
Rock type	LSB	LSB	HSB	HSB	HSB	HSB	HSB	HSB	HSB	HSB	HSB	HSB	HSB	HSB	HSB	HSB	HSB	HMA	HMA	HMA	LSB	LSB	LSB	LSB	HSB	HSB	HSB	HSB	HSB	HSB	HSB	HSB	HSB	HSB	HSB
Analysis	111-3-op	111-6	#80-2 [C]	#80-1 [C]	#80-4 [R]	#80-5 [C]	#88-3	#88-4	#88-5	#88-6	#88-9	#88-12	#88-10	#88-11	#89-3	#89-4	#89-9	#90-1 [C]	#90-2 [R]	#90-6 [C]	#203-3	#203-4	191-1	191-5	182-2 [C]	182-4 [C]	182-5 [R]	182-6 [R]	182-8 [C]	182-9 [R]	182-10 [R]	183-1 [C]	185-4	185-9	188-1	188-2
SiO2	55.65	55.54	57.21	57.48	57.03	57.74	56.51	57.19	57.22	56.55	56.18	57.22	54.37	56.48	56.25	56.40	56.70	57.01	55.69	55.36	55.22	58.14	57.74	57.45	56.86	56.76	55.66	56.98	56.96	56.36	56.80	57.48	57.48	57.60	57.99	57.19
TiO2	0.05	0.06	0.03	0.02	0.04	0.04	0.05	0.02	0.03	0.05	0.01	0.03	0.06	0.03	0.04	0.02	0.04	0.03	0.05	0.08	0.11	0.05	0.03	0.03	0.06	0.05	0.05	0.04	0.04	0.04	0.04	0.02	0.04	0.03	0.04	0.06
Al2O3	0.73	1.37	0.99	0.89	1.11	1.06	1.19	0.56	0.84	0.99	0.26	0.73	0.56	0.68	0.95	1.24	1.14	0.92	1.28	1.90	1.45	0.72	0.84	1.08	1.07	0.97	1.06	1.32	1.05	0.96	1.09	0.86	0.86	1.04	0.89	0.44
FeO	8.26	7.99	7.52	7.09	7.91	7.57	10.07	8.55	8.03	9.74	14.38	7.91	16.92	8.35	9.18	9.36	7.80	8.84	9.68	10.98	13.11	7.66	7.47	7.39	8.47	9.06	12.41	8.25	7.76	11.30	7.78	7.24	7.69	7.34	6.71	10.28
Cr2O3	0.35	0.70	0.55	0.53	0.52	0.50	0.23	0.46	0.62	0.29	0.12	0.57	0.05	0.39	0.45	0.36	0.90	0.46	0.40	0.22	0.07	0.55	0.44	0.58	0.37	0.55	0.23	0.48	0.70	0.31	0.63	0.63	0.39	0.56	0.61	0.12
MnO	0.26	0.19	0.20	0.17	0.15	0.16	0.21	0.23	0.17	0.24	0.39	0.19	0.40	0.20	0.22	0.21	0.19	0.18	0.26	0.20	0.23	0.21	0.20	0.18	0.24	0.20	0.25	0.18	0.20	0.28	0.18	0.21	0.18	0.14	0.15	0.32
NiO	0.05	0.04	0.12	0.09	0.10	0.09	0.09	0.04	0.07	0.06	0.08	0.09	0.04	0.09	0.05	0.05	0.08	0.08	0.06	0.06	0.05	0.03	0.07	0.08	0.09	0.04	0.03	0.06	0.09	0.05	0.09	0.07	0.12	0.09	0.06	0.05
MgO	31.10	30.50	31.95	32.30	31.65	32.24	29.71	30.29	31.45	29.57	28.30	31.98	25.37	31.24	30.59	30.21	31.12	31.26	29.97	28.35	27.36	31.26	32.72	32.64	31.20	31.01	28.78	31.83	32.34	29.59	32.48	32.86	32.30	32.58	33.85	29.90
CaO	2.90	2.78	1.49	1.33	1.62	1.51	2.07	2.80	1.46	2.28	0.31	1.45	0.97	1.56	1.52	1.84	1.65	1.60	1.85	2.74	1.76	2.21	1.40	1.42	1.96	2.04	1.56	1.54	1.35	1.81	1.40	1.11	1.60	1.42	0.43	2.26
Na2O	0.02	0.01	0.01	0.02	0.02	0.02	b.d.	0.04	0.03	0.01	0.02	0.03	b.d.	0.02	0.03	b.d.	0.04	0.03	0.03	0.04	0.02	0.02	0.01	0.02	0.05	0.02	0.00	0.01	0.01	b.d.	0.01	b.d.	0.02	b.d.	0.03	0.02
K2O	b.d.	b.d.	0.01	0.01	0.01	0.01	b.d.	b.d.	0.01	0.01	b.d.	b.d.	b.d.	b.d.	0.01	0.01	b.d.	b.d.	b.d.	b.d.	b.d.	b.d.	b.d.	b.d.	b.d.	b.d.	0.01	0.01	b.d.	b.d.	0.01	b.d.	b.d.	b.d.	b.d.	b.d.
Total	99.37	99.18	100.08	99.93	100.16	100.94	100.13	100.18	99.93	99.79	100.05	100.20	98.74	99.04	99.29	99.70	99.66	100.41	99.27	99.93	99.38	100.85	100.92	100.87	100.37	100.70	100.04	100.70	100.50	100.70	100.51	100.48	100.68	100.80	100.76	100.64
Number of cations on the basis of 6(O)																																			
Si	1.961	1.964	1.996	2.004	1.991	1.996	1.995	2.010	2.005	2.003	2.014	1.996	2.005	1.997	1.992	1.992	1.993	1.992	1.978	1.968	1.990	2.021	1.993	1.984	1.986	1.981	1.982	1.979	1.978	1.985	1.971	1.991	1.992	1.991	1.994	2.010
Al	0.030	0.057	0.041	0.037	0.046	0.044	0.049	0.023	0.035	0.041	0.011	0.030	0.024	0.029	0.039	0.052	0.048	0.038	0.053	0.080	0.062	0.029	0.034	0.044	0.044	0.040	0.044	0.054	0.043	0.040	0.044	0.035	0.035	0.043	0.036	0.018
Ti	0.001	0.002	0.001	0.001	0.001	0.001	0.001	0.001	0.001	0.001	0.000	0.001	0.002	0.001	0.001	0.001	0.001	0.001	0.001	0.002	0.003	0.001	0.001	0.001	0.002	0.001	0.001	0.001	0.001	0.001	0.001	0.001	0.001	0.001	0.001	0.002
Fe3	0.036	0.000	0.000	0.000	0.000	0.000	0.000	0.000	0.000	0.000	0.000	0.000	0.000	0.000	0.000	0.000	0.000	0.000	0.000	0.000	0.000	0.000	0.000	0.000	0.000	0.000	0.000	0.000	0.000	0.000	0.000	0.000	0.000	0.000	0.000	0.000
Fe2	0.207	0.236	0.219	0.207	0.231	0.219	0.297	0.251	0.235	0.288	0.431	0.231	0.522	0.247	0.272	0.277	0.229	0.258	0.287	0.326	0.395	0.223	0.216	0.213	0.247	0.264	0.370	0.240	0.225	0.333	0.226	0.210	0.223	0.212	0.193	0.302
Mg	1.634	1.608	1.662	1.679	1.647	1.662	1.563	1.586	1.642	1.562	1.513	1.662	1.394	1.647	1.614	1.591	1.631	1.628	1.586	1.502	1.470	1.620	1.684	1.680	1.625	1.613	1.528	1.648	1.674	1.554	1.680	1.697	1.669	1.679	1.736	1.566
Cr	0.010	0.020	0.015	0.015	0.014	0.014	0.006	0.013	0.017	0.008	0.003	0.016	0.001	0.011	0.013	0.010	0.025	0.013	0.011	0.006	0.002	0.015	0.012	0.016	0.010	0.015	0.006	0.013	0.019	0.009	0.017	0.017	0.011	0.015	0.017	0.003
Ni	0.001	0.001	0.003	0.003	0.003	0.003	0.003	0.001	0.002	0.002	0.002	0.003	0.001	0.003	0.001	0.001	0.002	0.002	0.002	0.002	0.001	0.001	0.002	0.002	0.003	0.001	0.001	0.002	0.003	0.001	0.003	0.002	0.003	0.003	0.002	0.001
Mn	0.008	0.006	0.006	0.005	0.004	0.005	0.006	0.007	0.005	0.007	0.012	0.006	0.012	0.006	0.007	0.006	0.006	0.005	0.008	0.006	0.007	0.006	0.006	0.005	0.007	0.006	0.008	0.005	0.006	0.008	0.005	0.006	0.005	0.004	0.004	0.010
Ca	0.110	0.105	0.056	0.050	0.061	0.056	0.078	0.105	0.055	0.087	0.012	0.054	0.038	0.059	0.058	0.070	0.062	0.060	0.070	0.104	0.068	0.082	0.052	0.053	0.073	0.076	0.060	0.057	0.050	0.068	0.052	0.041	0.059	0.053	0.016	0.085
Na	0.001	0.001	0.001	0.001	0.001	0.001	0.000	0.003	0.002	0.001	0.001	0.002	0.000	0.001	0.002	0.000	0.003	0.002	0.002	0.003	0.001	0.001	0.001	0.001	0.003	0.001	0.000	0.001	0.001	0.000	0.001	0.000	0.001	0.000	0.002	0.001
K	0.000	0.000	0.000	0.000	0.000	0.000	0.000	0.000	0.000	0.000	0.000	0.000	0.000	0.000	0.000	0.000	0.000	0.000	0.000	0.000	0.000	0.000	0.000	0.000	0.000	0.000	0.000	0.000	0.000	0.000	0.000	0.000	0.000	0.000	0.000	0.000
Cations	4.000	4.000	4.000	4.000	4.000	4.000	4.000	4.000	4.000	4.000	4.000	4.000	4.000	4.000	4.000	4.000	4.000	4.000	4.000	4.000	4.000	4.000	4.000	4.000	4.000	4.000	4.000	4.000	4.000	4.000	4.000	4.000	4.000	4.000	4.000	4.000
Mg#	*0.89*	*0.87*	*0.88*	*0.89*	*0.88*	*0.88*	*0.84*	*0.86*	*0.87*	*0.84*	*0.78*	*0.88*	*0.73*	*0.87*	*0.86*	*0.85*	*0.88*	*0.86*	*0.85*	*0.82*	*0.79*	*0.88*	*0.89*	*0.89*	*0.87*	*0.86*	*0.81*	*0.87*	*0.88*	*0.82*	*0.88*	*0.89*	*0.88*	*0.89*	*0.90*	*0.84*

Notes: C, R (in square brackets) = cores, rims.
Abbreviations: HMA, high magnesium andesite; HSB, high silica boninite; LSB, low silica boninite.

Whattam et al. (2020)

Supplementary Table S4 Chemical compositions of olivine

Drill hole	**U1439C**									**U1442A**			
Rock type	LSB	LSB	LSB	LSB	LSB	HSB	HSB	HSB	HSB	HSB	HSB	HSB	HSB
Analysis	#103-1 [C]	111-1 [C]	111-2 [R]	111-5 [C]	137-1 [C]	#88-1 [C]	#88-2 [R]	#89-1 [C]	#89-2 [R]	185-1 [C]	185-2 [R]	185-6	196-2 [R]
SiO_2	41.41	40.43	39.73	40.87	40.00	41.31	41.48	41.34	41.34	41.62	41.17	40.48	41.47
TiO_2	b.d.	0.02	0.02	0.01	0.01	b.d.	0.01	b.d.	b.d.	b.d.	b.d.	b.d.	0.01
Al_2O_3	0.03	0.01	0.04	0.02	0.01	0.02	b.d.	0.02	0.02	b.d.	b.d.	b.d.	0.05
FeO	10.26	7.99	11.20	8.62	8.89	9.87	8.25	9.06	9.19	8.23	11.04	12.44	9.45
MnO	0.20	0.10	0.18	0.14	0.15	0.16	0.15	0.18	0.15	0.11	0.18	0.19	0.14
MgO	48.34	50.35	47.92	49.34	49.17	47.88	49.22	48.52	48.67	50.16	47.61	46.90	49.07
CaO	0.15	0.15	0.21	0.16	0.17	0.13	0.12	0.13	0.12	0.13	0.12	0.18	0.16
Na_2O	0.01	b.d.	b.d.	b.d.	0.01	0.01	b.d.	b.d.	b.d.	b.d.	b.d.	0.01	b.d.
K_2O	b.d.	b.d.	b.d.	b.d.	0.01	b.d.	0.01	b.d.	b.d.	b.d.	b.d.	b.d.	b.d.
NiO	0.25	0.31	0.15	0.32	0.23	0.35	0.39	0.23	0.24	0.32	0.28	0.25	0.22
Total	100.65	99.36	99.45	99.48	98.65	99.73	99.63	99.48	99.73	100.57	100.40	100.45	100.57
Number of cations on the basis of 4(O)													
Si	1.010	0.991	0.988	1.002	0.992	1.015	1.013	1.014	1.012	1.007	1.010	1.000	1.008
Al	0.001	0.000	0.001	0.001	0.000	0.001	0.000	0.001	0.001	0.000	0.000	0.000	0.001
Ti	0.000	0.000	0.000	0.000	0.000	0.000	0.000	0.000	0.000	0.000	0.000	0.000	0.000
Fe^2	0.209	0.164	0.233	0.177	0.184	0.203	0.168	0.186	0.188	0.166	0.226	0.257	0.192
Mn	0.004	0.002	0.004	0.003	0.003	0.003	0.003	0.004	0.003	0.002	0.004	0.004	0.003
Mg	1.757	1.840	1.776	1.804	1.818	1.753	1.792	1.774	1.776	1.809	1.741	1.728	1.778
Ca	0.004	0.004	0.006	0.004	0.005	0.003	0.003	0.003	0.003	0.003	0.003	0.005	0.004
Na	0.000	0.000	0.000	0.000	0.000	0.000	0.000	0.000	0.000	0.000	0.000	0.000	0.000
K	0.000	0.000	0.000	0.000	0.000	0.000	0.000	0.000	0.000	0.000	0.000	0.000	0.000
Ni	0.005	0.006	0.003	0.006	0.005	0.007	0.008	0.005	0.005	0.006	0.006	0.005	0.004
Cations	2.990	3.007	3.011	2.997	3.007	2.985	2.987	2.987	2.988	2.993	2.990	2.999	2.990
Mg#	*0.89*	*0.92*	*0.88*	*0.91*	*0.91*	*0.90*	*0.91*	*0.91*	*0.90*	*0.92*	*0.89*	*0.87*	*0.90*

Notes: b.d. = below detection limits, Mg# = $Mg/(Mg+Fe^{2+})$, C, R (in square brackets) = cores, rims.
Abbreviations: HSB, high silica boninite; LSB, low silica boninite.

Supplementary Table S5 Chemical compositions of spinel

Drill hole	**U1440B**	**U1439C**			**U1442A**						
Rock type	FAB	LSB	LSB	HSB	LSB	LSB	HSB	HSB	HSB	HSB	HSB
Analysis	37-2-13	#103-8	111-9	#89-7	191-3	191-6	185-3	185-7	196-3	196-4	#196-6
SiO_2	0.24	0.39	0.17	0.23	0.18	0.16	0.54	0.15	0.19	0.18	0.07
TiO_2	17.11	0.20	0.20	0.07	0.11	0.11	0.06	0.13	0.16	0.19	0.18
Al_2O_3	2.75	9.42	8.32	6.90	9.45	9.82	8.78	9.49	9.36	10.32	9.77
Cr_2O_3	0.12	55.73	58.88	60.26	55.99	56.19	59.24	55.79	57.41	56.22	57.97
MnO	0.37	0.21	0.21	0.21	0.19	0.22	0.17	0.23	0.24	0.16	0.19
MgO	0.69	10.74	11.15	10.19	11.12	11.12	12.55	10.72	11.94	12.00	12.09
NiO	0.02	0.09	0.10	0.10	0.10	0.11	0.12	0.09	0.09	0.09	0.09
FeO	69.49	16.37	15.65	16.59	15.82	16.14	13.48	16.69	14.62	14.60	15.22
Fe_2O_3		5.48	3.97	3.51	5.80	5.81	4.07	6.27	4.89	4.55	5.39
Total	90.96	98.63	98.65	98.06	98.76	99.70	99.01	99.56	98.91	98.31	100.97
Number of cations on the basis of 4(O)											
Cr		1.479	1.561	1.628	1.477	1.468	1.552	1.465	1.504	1.474	1.486
Ti		0.005	0.005	0.002	0.003	0.003	0.001	0.003	0.004	0.005	0.004
Al		0.373	0.329	0.278	0.372	0.382	0.343	0.372	0.366	0.403	0.374
Fe^3		0.138	0.100	0.090	0.146	0.145	0.102	0.157	0.122	0.114	0.132
Fe^2		0.459	0.439	0.474	0.441	0.446	0.374	0.464	0.405	0.405	0.413
Mn		0.006	0.006	0.006	0.006	0.006	0.005	0.006	0.007	0.005	0.005
Mg		0.537	0.557	0.519	0.553	0.548	0.620	0.531	0.590	0.593	0.584
Ni		0.002	0.003	0.003	0.003	0.003	0.003	0.002	0.003	0.002	0.002
Cations		3.000	3.000	3.000	3.000	3.000	3.000	3.000	3.000	3.000	3.000
Mg#		*0.54*	*0.56*	*0.52*	*0.56*	*0.55*	*0.62*	*0.53*	*0.59*	*0.59*	*0.59*
Cr#		*0.80*	*0.83*	*0.85*	*0.80*	*0.79*	*0.82*	*0.80*	*0.80*	*0.79*	*0.80*

Note: Mg# = $Mg/(Mg+Fe^{2+})$, Cr#=Cr/(Cr+Al).

Abbreviations: FAB, forearc basalt; HSB, high silica boninite; LSB, low silica boninite.

Supplementary Table S6 Chemical compositions of plagioclase

| Drill hole | U1439C | | | | | U1442A | | | | |

Table S7 P-T calculations based on clinopyroxene thermobarometry.

Sample-spot	Rock Type	Mineral	$K_D(Fe\text{-}Mg)^{cpx\text{-}liq*}$	P (kbar)	±	T (°C)	±	Ref.
#35-area2-1	FAB	cpx	0.26	0.8		1135		1
				0.9		1173		2
				1.0		1149		3
				-		1144		4
				0.9	**0.1**	**1150**	**8**	
#35-area1-2	FAB	cpx	0.27	1.2		1135		1
				1.1		1170		2
				1.2		1148		3
				-		1148		4
				1.2	**0.0**	**1150**	**6**	
#73-area1-1	FAB	cpx	0.28	2.7		1203		1
				4.1		1211		2
				-		1110		3
				-		1146		4
				3.4	**0.7**	**1167**	**29**	
#73-area1-3core	FAB	cpx	0.27	4.1		1214		1
				5.2		1222		2
				-		1122		3
				-		1158		4
				4.6	**0.5**	**1179**	**28**	
#73-area2-9	FAB	cpx	0.28	2.2		1199		1
				3.8		1207		2
				-		1104		3
				-		1141		4
				3.0	**0.8**	**1163**	**29**	
#73-area3-11	FAB	cpx	0.28	2.6		1203		1
				4.1		1211		2
				-		1108		3
				-		1145		4
				3.4	**0.7**	**1167**	**18**	
164-2	FAB	cpx	0.27	0.3		1154		1
				0.5		1172		2
				0.7		1114		3
				-		1128		4
				0.5	**0.2**	**1142**	**13**	
164-4	FAB	cpx	0.27	1.4		1165		1
				1.4		1186		2
				1.8		1135		3
				-		1137		4
				1.5	**0.2**	**1156**	**14**	
164-5	FAB	cpx	0.27	1.9		1168		1
				1.7		1186		2
				2.2		1135		3
				-		1142		4
				2.0	**0.2**	**1158**	**13**	
180-7	FAB	cpx	0.28	3.3		1198		1
				3.9		1225		2
				3.6		1166		3
				-		1173		4
				3.6	**0.1**	**1190**	**13**	
172-1	FAB	cpx	0.27	0.8		1185		1
				2.4		1224		2
				1.9		1149		3
				-		1143		4
				1.7	**0.6**	**1175**	**21**	

Notes: *$K_{D(}Fe\text{-}Mg)^{cpx\text{-}liq}$ calculated from Eqn. 35, Putirka et al. (2008). $K_D(Fe\text{-}Mg)^{cpx\text{-}basaltic\ melt}$ = 0.23 ± 0.05 (Toplis and Carroll, 1995). Abbreviations: AND, Andesite; BB, basaltic boninite; FAB, forearc basalt. Reference key: 1, Eqns. P1, T1 (P, T), Putirka et al. (1996); 2, Putirka et al. (2003); 3, Eqns. 30, 33 (P, T), Putirka (2008); 4, Eqn. 34 (T), Putirka (2008). Bold numbers represent the mean and STDEV of the 3 or 4 P or T listed above. The mean P and T of all means obtained on discrete sample-spots (in bold) for the FAB are: 2.4 ± 0.4 kbar & 1164 ± 7°C (FAB). See also Table 3.
Model uncertanties associated with estimated P and T are ± 1 kbar and ± 30°C, respectively.

Whattam et al. (2020)

Table S8 P-T calculations based on orthopyroxene thermobarometry.

Sample-spot	Rock Type	Mineral	$K_D(Fe\text{-}Mg)^{opx\text{-}liq}$	P(kbar)	±	Ref.	T (°C)	±	Ref.
#90-1	HMA	opx	0.28	0.1		1	1228		4
				0.4		2	1195		5
				0.1		3	1155		6
				0.2	**0.05**		**1193**	**26**	
191-1	LSB	opx	*0.37*	0.7		1	1304		4
				0.8		2	1296		5
				0.5		3	1298		6
				0.7	**0.1**		**1299**	**3**	
191-5	LSB	opx	*0.36*	0.8		1	1304		4
				0.8		2	1296		5
				0.5		3	1298		6
				0.7	**0.2**		**1299**	**3**	
#203-4	LSB	opx	0.31	0.4		1	1216		4
				0.5		2	1227		5
				0.1		3	1198		6
				0.3	**0.1**		**1214**	**9**	
#88-4	HSB	opx	*0.36*	0.4		1	1268		4
				0.5		2	1233		5
				0.3		3	1206		6
				0.4	**0.1**		**1236**	**31**	
88-5 [C]	HSB	opx	0.32	0.3		1	1268		4
				0.6		2	1235		5
				0.1		3	1206		6
				0.3	**0.1**		**1236**	**31**	
#88-11	HSB	opx	0.34	0.2		1	1268		4
				0.5		2	1230		5
				0.1		3	1206		6
				0.2	**0.1**		**1235**	**31**	
#89-3	HSB	opx	*0.39*	0.3		1	1268		4
				0.6		2	1219		5
				0.1		3	1207		6
				0.4	**0.1**		**1231**	**30**	
#89-9	HSB	opx	0.32	0.3		1	1268		4
				0.4		2	1237		5
				0.0		3	1207		6
				0.3	**0.1**		**1237**	**30**	
182-2 [C]	HSB	opx	*0.37*	0.5		1	1291		4
				0.8		2	1252		5
				0.4		3	1225		6
				0.6	**0.1**		**1256**	**33**	
182-4 [C]	HSB	opx	*0.39*	0.3		1	1291		4
				0.4		2	1258		5
				0.2		3	1225		6
				0.3	**0.1**		**1258**	**33**	
182-8	HSB	opx	0.32	0.2		1	1291		4
				-		2	1258		5
				0.2		3	1225		6
				0.2	**0.005**		**1258**	**33**	
183-1 [C]	HSB	opx	0.30	-		1	1293		4
				0.5		2	1265		5
				0.2		3	1228		6
				0.3	**0.2**		**1262**	**32**	
188-1 [*C*]	HSB	opx	0.30	0.4		1	1297		4
				0.6		2	1261		5
				0.1		3	1234		6
				0.4	**0.2**		**1264**	**32**	

Notes:

*$K_D(Fe\text{-}Mg)^{opx\text{-}basaltic\ melt}$ = 0.29 ± 0.06 (see Putirka, 2008).

Bold text demarcates the mean and STDEV of the above listed P & T.

Abbreviations: Eqn., Equation; HMA, high magnesium andesite; HSB, high silica boninite; LSB, low silica boninite

Reference key: 1, 2, 3, Eqns. 29a, 29b, 29c, respectively of Putrika (2008); 4, Beattie (1993);
5, 6, Eqns. 28a, 28b, respectively, of Putirka (2008). Note the sample numbers in italics are ones which yield KD(Fe-Mg) outside of the bounds of error and so are not used in the calculation of mean T and P estimates.

The mean P & T of all means obtained on discrete spots for the LSB and HSB are 0.3 ± 0.1 kbar, 1214 ± 9 °C and 0.3 ± 0.1 kbar, 1248 ± 7 °C, respectively.

Whattam et al. (2020)

Table S9 Temperature calculations based on olivine thermometry.

Drill core	Sample-spot	Rock Type	Mineral	Core/rim	T (°C)	±	Ref.
n.a.	#103-1	LSB	olivine	C	**1119**		1
	111-calc 1	LSB	olivine	C	**1185**		1
	137-calc1	LSB	olivine	C	**1158**		1
	88 calc 1	HSB	olivine	C	**1142**		1
	#89-1	HSB	olivine	C	**1158**		1
	185-1	HSB	olivine	C	**1190**		1
	196-1	HSB	olivine	C	**1141**		1
U1439A 21X-CC 22/25	Olivine 1	HSB	olivine	core	1125		1
		HSB	olivine	core	1124		1
		HSB	olivine	core	1125		1
		HSB	olivine	core	1125		1
		HSB	olivine	core	1125		1
		HSB	olivine	core	1125		1
		HSB			**1125**	**0.2**	
		HSB	olivine	rim	1127		1
		HSB	olivine	rim	1130		1
		HSB			**1128**	**2**	
	Olivine 2	HSB	olivine	core	1129		1
		HSB	olivine	core	1124		1
		HSB	olivine	core	1124		1
		HSB			**1126**	**3**	
U1442A 17R-1 61/65	Olivine 1	HSB	olivine	core	1136		1
		HSB	olivine	core	1136		1
		HSB	olivine	core	1136		1
		HSB	olivine	core	1138		1
		HSB	olivine	core	1139		1
		HSB	olivine	core	1139		1
		HSB	olivine	core	1140		1
		HSB	olivine	core	1140		1
		HSB	olivine	core	1140		1
		HSB	olivine	core	1140		1
		HSB	olivine	core	1140		1
		HSB	olivine	core	1140		1
		HSB	olivine	core	1140		1
		HSB			**1139**	**2**	
	Olivine 1	HSB	olivine	rim	1140		1
		HSB	olivine	rim	1145		1
		HSB			**1143**	**3**	
U1442A 21R-2 1/4	Olivine 1	HSB	olivine	core	1188		1
		HSB	olivine	core	1189		1
		HSB	olivine	core	1188		1
		HSB	olivine	core	1188		1
		HSB	olivine	core	1188		1
		HSB	olivine	core	1188		1
		HSB	olivine	core	1188		1
		HSB	olivine	core	1188		1
		HSB	olivine	core	1188		1
		HSB	olivine	core	1188		1
		HSB	olivine	core	1188		1
		HSB	olivine	core	1188		1
		HSB	olivine	core	1187		1
		HSB	olivine	core	1187		1
		HSB			**1188**	**0.4**	
U1442A 26R-1 54/58	Olivine 1	HSB	olivine	core	1160		1
		HSB	olivine	core	1161		1
		HSB	olivine	core	1161		1
		HSB	olivine	core	1161		1
		HSB	olivine	core	1161		1
		HSB	olivine	core	1161		1
		HSB	olivine	core	1163		1
		HSB	olivine	core	1161		1
		HSB	olivine	core	1161		1
		HSB	olivine	core	1160		1
		HSB	olivine	core	1161		1
		HSB			**1161**	**0.7**	
U1439C 19R-4 84/87	Olivine 2	LSB	olivine	core	1181		1
		LSB	olivine	core	1181		1
		LSB	olivine	core	1182		1
		LSB			**1181**	**0.3**	
	Olivine 3	LSB	olivine	core	1181		1
		LSB	olivine	core	1182		1
		LSB	olivine	core	1182		1
		LSB			**1182**	**0.2**	
	Olivine 4	LSB	olivine	core	1182		1
		LSB	olivine	core	1181		1
		LSB	olivine	core	1182		1
		LSB	olivine	core	1181		1
		LSB			**1182**	**0.4**	
	Olivine 1	LSB	olivine	core	1201		1
		LSB	olivine	core	1202		1
		LSB	olivine	core	1202		1
		LSB	olivine	core	1203		1
		LSB	olivine	core	1204		1
		LSB			**1202**	**1**	
U1439C 29R-4 113/117	Olivine 2	LSB	olivine	core	1150		1
		LSB	olivine	core	1152		1
		LSB			**1151**	**1**	
	Olivine 1	LSB	olivine	core	**1161**		1
		LSB					
U1439C 30R-1 4/5	Olivine 1	LSB	olivine	core	1160		1
		LSB	olivine	core	1160		1
		LSB	olivine	core	1159		1
		LSB			**1160**	**1**	
U1439C 33R-1 114/120	Olivine 1	LSB	olivine	core	1191		1
		LSB	olivine	core	1190		1
		LSB	olivine	core	1191		1
		LSB	olivine	core	1190		1
		LSB	olivine	core	1190		1
		LSB	olivine	core	1192		1
		LSB			**1190**	**1**	
	Olivine 2	LSB	olivine	core	1187		1
		LSB	olivine	core	1187		1
		LSB			**1187**	**0.2**	

Notes: *KD(Fe-Mg)olivine-basaltic melt = 0.30 ± 0.03 (Roeder and Emslie, 1970; Putirka, 2016).
Bold text demarcates mean and standard deviation of the five temperatures listed above.
Abbreviations: HSB, high silica boninite; LSB, low silica boninite. All temperatures were calculated using adjusted whole rock compositions (see text) using Eqn. 22 of Putirka (2008, Ref. 1).
The mean temperatures of the LSB and HSB are 1172±23^{o}C and 1152±24.^{o}C

Whattam et al. (2020)

Supplementary Table S10 PetDB MORB samples in in equilibrium and their P & T estimates on the basis of clinopyroxene thermobarometry

Sample	Material	Mg#-WR	Mg#-cpx	KD(Fe-Mg)	Temperature (°C)	Pressure (kbar)
AGU0032-005-001	GL	60	83	0.28	1180	-0.3
AGU0032-005-002	GL	61	85	0.28	1183	0.6
AII0032-3-011-046	WR	63	84	0.28	1192	3.7
AII0032-3-011-102	WR	61	83	0.28	1181	3.3
AII0032-3-012-006	GL	65	85	0.28	1196	3.1
AII0073-1-013-001C	GL	65	85	0.29	1197	0.6
AII0107-6-033-027	GL	51	79	0.27	1152	1.6
ALV0830-005	GL	64	88	0.29	1220	4.5
ALV0912-R006	GL	62	85	0.28	1188	0.9
ALV0919-R001	GL	62	83	0.29	1197	3.6
ALV1550-004	GL	66	89	0.29	1188	0.9
ALV1555-001	GL	63	84	0.29	1200	2.0
ALV2697-005	GL	60	85	0.28	1172	-1.5
ALV4084-1847	WR	62	83	0.29	1189	1.9
ARP1973-010-002	GL	54	79	0.28	1169	0.4
ATN0011-23-020705-1146	WR	60	82	0.28	1198	0.4
CHN0115-4-005-001	GL	45	75	0.27	1133	3.4
CHR0031-003-356	GL	68	89	0.28	1179	-1.1
CHRSR01-002-102	GL	59	85	0.28	1186	2.2
CHRSR01-002-201	GL	59	82	0.28	1194	2.1
CHRSR01-006-101	WR	57	81	0.28	1200	2.0
CON2802-014-001	GL	61	85	0.28	1190	0.4
CON2802-015-002	GL	60	86	0.28	1193	1.3
CON2802-015-004	GL	59	85	0.28	1183	-0.3
CON2802-016-002	GL	62	85	0.29	1212	3.4
CON2802-022-004	WR	63	84	0.29	1204	2.4
CYA1978-002-001	GL	59	83	0.28	1180	1.6
CYA1978-004-007	GL	63	86	0.29	1201	2.6
CYA1978-004-007A	GL	62	85	0.29	1223	1.9
CYA1978-009-015	GL	62	86	0.29	1196	2.1
CYA1978-019-069	WR	61	85	0.29	1197	1.9
CYA1978-019-070	GL	62	87	0.28	1181	1.5
CYA1984-030-006	GL	61	85	0.29	1196	2.4
DSDP065-0485A-012-001/076-082	WR	55	79	0.28	1165	0.5
ENVCSM3-CSM3	GL	62	84	0.28	1174	0.1
GIL0103-035-022	GL	62	83	0.29	1221	4.8
GIL0104-002-004	GL	60	84	0.29	1205	1.8
GIL0104-007-001A	GL	56	82	0.28	1189	3.8
GIL1979-007-001	GL	58	81	0.28	1197	2.3
GLJ-010	GL	55	82	0.28	1164	0.0
LEE81WF-11-008-002	WR	62	85	0.28	1188	1.2
MELPROT-5-037-001	WR	67	87	0.27	1188	8.3
MELPROT-5-037-003	WR	69	89	0.28	1204	5.1
MET41/2-166-001	GL	51	79	0.28	1155	1.6
MET41/2-173-001	GL	51	81	0.27	1145	-0.2
MET41/2-190-001	GL	46	78	0.27	1143	-0.3
ODP0309-1256D-075R-001/076-080	WR	54	82	0.28	1175	0.6
ODP0309-1256D-077R-001/069-073	WR	55	83	0.28	1159	-0.2
ODP0309-1256D-088R-001/001-005	WR	57	85	0.28	1168	0.9
ODP0309-1256D-099R-002/005-009	WR	59	85	0.28	1172	-0.6
ODP0309-1256D-101R-001/116-120	WR	60	85	0.28	1166	-1.3
ODP0309-1256D-106R-001/077-080	WR	61	85	0.29	1203	1.3
ODP0309-1256D-121R-001/002-005	WR	59	84	0.28	1168	0.2
ODP0309-1256D-143R-002/050-053	WR	58	86	0.28	1163	-0.9
ODP0309-1256D-161R-001/000-004	WR	56	84	0.29	1180	1.1
PS4CSM4-1504-002	GL	59	85	0.28	1154	-0.5
PS4CSM4-1505-001	GL	59	85	0.28	1138	-1.3
SON0012-033-D001	GL	47	79	0.28	1175	1.6
SON0012-130-001	GL	47	74	0.29	1169	0.0
SON0012-190-001	GL	53	78	0.28	1144	-1.8
SON0012-193-001	GL	57	83	0.28	1191	1.9
SON0012-207-001	GL	58	82	0.28	1184	1.7
SON0012-228-D002	GL	55	79	0.28	1190	1.5
SON0157-017-001	GL	53	82	0.28	1158	0.7
SON0157-017-003	GL	54	82	0.28	1163	1.1
TRI0119-007-010	GL	69	90	0.29	1212	1.8
TRI0139-006-002	GL	52	78	0.30	1240	5.4
TRI0139-007-001	GL	58	85	0.29	1191	1.7
TRI0139-015-001	GL	56	82	0.29	1174	0.6
TRI0139-021-001	GL	43	75	0.30	1168	0.7
TRI0139-023-001	GL	56	81	0.31	1223	3.2
TRI0154-021-003	GL	63	86	0.28	1142	0.5
TRI0164-016-001	GL	55	81	0.28	1158	-0.4
TRI0164-024-003	GL	53	79	0.28	1170	1.3
WASCENT-001	GL	53	82	0.28	1151	0.0
			mean		**1182 ± 15**	**1.4 ± 0.2**
			min	0.27	1133	-1.8
			max	0.31	1240	8.3

Notes: P and T calculated on the basis of the barometer of Neave and Putirka (2017) and the thermometer of Putirka (2008, Eqn. 33), respectively.
Abbreviations: GL, glass; WR, whole-rock
Notes: *KD(Fe-Mg)olivine-basaltic melt = 0.30 ± 0.03 (Roeder and Emslie, 1970).

Supplementary Table S11 Fugacity calculations for Expedition 352 boninites.

Sample	boninite type	$\Delta \log f O_2$ FMQ
103	low-Si	0.88
111	low-Si	0.80
137	low-Si	0.17
89	high-Si	0.05
185	high-Si	0.38
196	high-Si	0.56
191	high-Si	1.04

Notes: Si, silica.

Whattam et al. (2020)

Supplementary Table S12 Boninite crystallization pressure and temperature estimates from the literature

Study	T(°C)	P (kbar)	Temperature determination method
Umino (1986)	1150-1215	-	uncertain
Crawford et al. (1989)	1150-1200	-	uncertain
Umino and Kushiro (1989)	1130-1315	- 0.8-1.6	melting experiments
van der Laan et al. (1989)	up to 1268	-	experimentally studied phase relations
van der Laan et al. (1992)	<1100-1260	1.0-2.5	phase diagram determination
Sobolev and Danyushevsky (1994)	1150-1390	0.15-1.7*	melt inclusion analysis
Acland (1996)	1100-1230	?	thermometry
Danyushevsky and Sobolev (1996)	<1300	-	uncertain
Dobson et al. (2006)	1080-1287	-	thermometry

* These pressures are to be interpreted with caution as melt inclusions not effective in estimating P relative cpx saturation; for this reason, these pressure estimates are not considered in the main text.

Whattam et al. (2020)